Si spreading in lattice-matched $In_{0.53}Ga_{0.47}As$ grown by molecular-beam epitaxy

E. Skuras and A. R. Long*
Department of Physics and Astronomy, Glasgow University, Glasgow G12 8QQ, United Kingdom

B. Vögele,† M. C. Holland, and C. R. Stanley
Department of Electronics and Electrical Engineering, Glasgow University, Glasgow G12 8QQ, United Kingdom

E. A. Johnson
Blackett Laboratory, Imperial College of Science, Technology and Medicine, Prince Consort Road, London SW7 2BZ, United Kingdom

M. van der Burgt, H. Yaguchi, and J. Singleton
Clarendon Laboratory, Department of Physics, University of Oxford, Parks Road, Oxford OX1 3PU, United Kingdom

(Received 27 May 1998; revised manuscript received 5 October 1998)

A detailed study is reported of Si spreading in slab- and δ-doped $In_{0.53}Ga_{0.47}As$ grown lattice matched to InP substrates by molecular beam epitaxy at temperatures from ≈ 420 to $\approx 520\,^{\circ}C$ and doping concentrations from 2×10^{12} to $1.5\times10^{13}\,cm^{-2}$. The spreading is deduced by comparing the individual subband densities calculated from a fast Fourier transform analysis of Shubnikov–de Haas measurements with those derived from self-consistent calculations for which the doping profile width is used as a fitting parameter. The growth conditions for the epitaxial layers were designed to differentiate between surface segregation and thermal diffusion of the dopant atoms. Surface segregation is found to be the dominant mechanism causing Si spreading at growth temperatures higher than $\approx 470\,^{\circ}C$. An ideal δ-doping profile in $In_{0.53}Ga_{0.47}As$ requires only the growth of a thin cap layer of undoped material at temperatures less than $\approx 470\,^{\circ}C$ over the δ doping. Holding the substrate temperature at values up to $\approx 520\,^{\circ}C$ during δ doping or the subsequent deposition of material over the cap does not produce any spreading. The three-band Kane model is found to provide an adequate description of the electronic properties of narrow Si doping profiles with carrier concentrations as high as $1.5\times10^{13}\,cm^{-2}$ and Fermi energies close to 550 meV, the separation between the Γ- and L-conduction band minima in $In_{0.53}Ga_{0.47}As$. The free electron concentrations from low magnetic field Hall measurements are consistently less than the sums of the individual subband densities derived from the Shubnikov–de Haas effect. In addition, for the same total Si doping density, the apparent electron concentration from Hall measurements is lower when the Si dopants are more confined compared with the case where the dopants are significantly spread. These apparent discrepancies are shown to follow from the different subband mobilities expected in these structures. From the data a direct measure of the standard deviation of carrier mobilities over subbands for a given structure is obtained. [S0163-1829(99)04515-4]

I. INTRODUCTION

δ doping is a technique employed in the epitaxial growth of semiconductors to achieve confinement of the dopant atoms to a single crystal plane of the host lattice.[1,2] In the case of the III-V materials, growth is suspended by interrupting the supply of group III atoms while the flux of the group V molecules is maintained on the surface. The required areal density of dopant atoms is deposited and then growth is resumed by reintroducing the group III atoms without the incident dopants. Careful control of the growth conditions is usually necessary during δ doping and when growth is resumed, to prevent the migration of the dopants away from the crystal plane on which they were deposited.[3–7] Thermal diffusion would cause Si donors to migrate from the original doping plane both towards the substrate and in the growth direction to form a symmetrical doping profile. For surface segregation only, an asymmetric doping profile resulting from preferential Si migration in the growth direction is expected.

Dopant distributions can be measured by two principal analytical methods, capacitance-voltage (CV) profiling[8] and secondary ion mass spectroscopy (SIMS).[9] A disadvantage of both CV and SIMS profiling is that neither can provide information on the pronounced two-dimensional electronic properties of the δ-doped region, only the total free charge or impurity density profile, respectively. The electronic subband structure can be calculated self-consistently by solving the one-dimensional Schrödinger and Poisson equations. These calculations, performed for either a uniform or a Gaussian distribution of Si donors in GaAs, show that the relative occupancies of the individual sub-bands are very sensitive to the width w_{Si} of the doping profile.[10–12] Since the individual sub-band densities $n_i\,(i=0,1,2,3\ldots)$ of a δ-doped sample can be determined with Shubnikov–de Haas (SdH) measurements and analysis of the SdH data by fast Fourier transform (FFT) techniques, spreading can be assessed indirectly by comparing the experimental values of n_i with those calculated self-consistently using w_{Si} as a fitting parameter.

In early studies based on this technique, the two-dimensional properties of Si δ-doped $In_{0.53}Ga_{0.47}As$ grown

on InP by molecular beam epitaxy (MBE) (Ref. 13) and metal-organic chemical vapor deposition (MOCVD) (Ref. 14) were demonstrated. Later studies[15] combined SdH with self-consistent calculations (SCC's) to infer that significant spreading of the Si donors away from the intended doping plane occurs in all Si δ-doped layers with nominal areal densities up to $4\times10^{12}\,\mathrm{cm}^{-2}$ when grown entirely at a substrate temperature $T_s\approx520\,^{\circ}\mathrm{C}$. In contrast, a near ideal δ-doping profile can be created when the δ layer is deposited at $T_s\approx470\,^{\circ}\mathrm{C}$ and covered by 20 monolayers (ML) of undoped material at the same substrate temperature, despite the subsequent growth of a 0.5 μm thick $In_{0.53}Ga_{0.47}As$ cap layer at $T_s\approx520\,^{\circ}\mathrm{C}$. This suggests that the most likely cause of Si spreading is surface segregation and that diffusion during growth at $T_s\approx520\,^{\circ}\mathrm{C}$ is negligible. A vital aspect of our initial work on Si-doped $In_{0.53}Ga_{0.47}As$ was to verify that when SdH measurements and SCC are combined the relative occupancies and therefore the spreading of Si deposited in thin slabs with a predetermined thickness can be accurately predicted. The agreement between the SdH and SCC results in this case was excellent when a uniform distribution of the Si donors was assumed with w_{Si} equal to the physical thickness of the slab.

In this paper our aims are as follows.

(i) To present a complete study of $In_{0.53}Ga_{0.47}As$ δ-doped layers designed to distinguish between dopant migration caused by thermal diffusion from spreading due to surface segregation.

(ii) To demonstrate that the interpretation of SdH data using SCC within the limitations of the three-band Kane model can be extended reliably to high doping densities with Fermi energies very close to the L minimum.

(iii) To show that in multi-sub-band systems with the same total donor density, the observed increasing discrepancy between the free electron densities deduced from Hall and SdH measurements associated with the progressive confinement of the doping profile is a direct consequence of the change in mobility distribution among the sub-bands.

II. EXPERIMENTAL TECHNIQUES

A. Molecular-beam epitaxy growth

The $In_{0.53}Ga_{0.47}As$ epitaxial layers were grown at 1 μm/h on semi-insulating Fe-InP(100) substrates in a Varian 3-inch Modular Gen II MBE system fitted with an arsenic cracker. An As_2 flux of approximately $1.9\times10^{15}\,\mathrm{cm}^{-2}\,\mathrm{s}^{-1}$ was used, corresponding to six times the minimum needed to grow GaAs at $T_s\approx580\,^{\circ}\mathrm{C}$ with an As-stable $(2\times4)(100)$ surface reconstruction. The $In_{0.53}Ga_{0.47}As$ surface was exposed to the As_2 flux throughout the growth of the structures, including the interrupts for the deposition of the Si δ layers and during the time required to lower and raise the substrate temperature. Additional information on the growth conditions was deduced from the surface reconstructions which changed from a (1×3) at $T_s\leqslant470\,^{\circ}\mathrm{C}$, through to a (2×3) for $470\leqslant T_s\leqslant500\,^{\circ}\mathrm{C}$ and a (2×4) for $T_s\geqslant500\,^{\circ}\mathrm{C}$, all referred to the $[1\bar{1}0]$ azimuth.[16] The Si effusion cell temperature was calibrated against both low magnetic field Hall and high magnetic field SdH measurements of the free electron concentration in a large number of uniformly doped GaAs and lattice matched InGaAs layers. For the δ-doped layers the same Si effusion cell temperature was used with the doping time during growth interrupt adjusted to provide the required Si sheet density.

B. Measurement and analysis

Shubnikov–de Haas measurements were performed in the dark at 1.2 K using a 13 T superconducting magnet or at 4.2 K using a 50 T pulsed magnetic field system.[17] Hall bars with 3:1 length to width ratio were fabricated with either electron beam or optical lithography. The SdH data were numerically differentiated, expressed in reciprocal magnetic field and frequency analyzed by fast Fourier transform techniques. The electron sub-band densities n_i $(i=0,1,2,3,\ldots)$ are related to the frequencies ν_i of the SdH oscillations by the expression $n_i=2e\nu_i/h$ assuming unresolved spin splitting, where e is the electronic charge and h is Planck's constant. The total free electron density n_s is the sum of the individual sub-band densities n_i of all the observed sub-bands, $n_s=\Sigma_i n_i$. Low magnetic field measurements of the Hall carrier concentration n_H were also performed at 4.2 K. This was invariably lower than the carrier concentration deduced from the SdH data, and the difference is the basis of the discussion in Sec. III D.

The electronic sub-band structure was calculated self-consistently by solving the one-dimensional Schrödinger and Poisson equations, and these calculations were performed assuming either a uniform distribution (UD) or a Gaussian distribution (GD) of Si donors in $In_{0.53}Ga_{0.47}As$. The nonparabolicity of the conduction band was included in the calculations within the limitations of the three-band Kane model.[18] The spreading of Si is assessed by comparing directly the individual sub-band densities deduced from the FFT analysis of the SdH data with those derived from SCC, with the width w_{Si} of the uniform dopant distribution or the full width at $1/e\times$ the maximum of the Gaussian doping profile as a fitting parameter. Though the applicability of the SCC would be enhanced by taking into account the asymmetry of the Si donor distribution caused by surface segregation, adequate agreement is generally obtained using the simpler approach.

III. RESULTS AND DISCUSSION

A. Layer structures and analysis of the dopant spreading

In this study, additional epitaxial layers with design were grown to provide conclusive and indisputable evidence of surface segregation of Si in $In_{0.53}Ga_{0.47}As$ at $T_s>470\,^{\circ}\mathrm{C}$. The layer configurations and growth temperatures of key samples are indicated diagrammatically in Fig. 1 and the measured parameters are summarized in Table I. Sample B603 is a typical structure δ doped with Si to a nominal areal density of $3.0\times10^{12}\,\mathrm{cm}^{-2}$ and grown entirely at $520\,^{\circ}\mathrm{C}$ to provide a reference for the extent of Si migration in $In_{0.53}Ga_{0.47}As$ grown under nominally optimum conditions. Layers B684 and B685 with intended δ-doping concentrations of $3.0\times10^{12}\,\mathrm{cm}^{-2}$ and B713 with $2.5\times10^{12}\,\mathrm{cm}^{-2}$ were grown with the following substrate temperature cycles to separate Si spreading towards the substrate from that migrating in the growth direction.

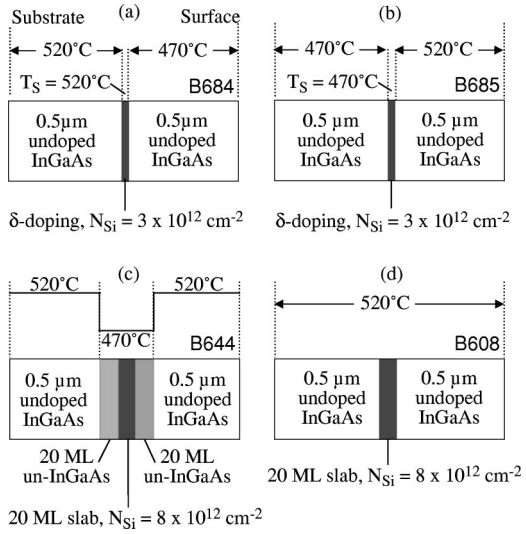

FIG. 1. Schematic layer structures and growth temperatures of key samples studied here: (a) B684, (b) B685, (c) B644, (d) B608. The layer structure of B713 was similar to that of B684, except that growth was interrupted for 15 min after the δ doping and before the temperature reduction for growth of the cap layer.

(i) B684 [Fig. 1(a)]: growth of 0.5 μm of undoped InGaAs and δ doping at 520 °C; a pause of 300 s to lower T_s to 470 °C; growth of a further 0.5 μm of undoped InGaAs at 470 °C.

(ii) B713: growth of 0.5 μm of undoped InGaAs and δ doping at 520 °C; a 15 min growth interrupt with the substrate temperature at 520 °C; a pause of 300 sec to lower T_s to 470 °C; growth of a final 0.5 μm of undoped InGaAs at 470 °C.

(iii) B685 [Fig. 1(b)]: growth of 0.5 μm of undoped InGaAs and δ doping at 470 °C; a pause of 300 s to raise T_s to 520 °C; growth of a further 0.5 μm of undoped InGaAs at 520 °C.

The only intentional difference between the growth cycles of B684 and B713 was the incorporation in B713 of a 15 min growth interrupt at 520 °C after the deposition of the Si δ layer. For layer B685 the temperature sequence applied to the growth of B684 was reversed, i.e., for B684 the growth of the 0.5 μm thick cap over the Si δ-doped layer was initiated at a relatively ''low'' temperature, whereas for B685 the wafer temperature was ''high'' at the comparable stage of the cycle.

Four occupied subbands are observed in the FFT amplitude spectrum of B603 with a total electron density 3.14 $\times 10^{12}\,\mathrm{cm}^{-2}$ and a subband ratio $n_{i=0}/n_{i=1}=2.16$. We showed in our earlier publication[15] that comparisons of this sub-band ratio for otherwise identical samples is a good measure of the width of the dopant distribution. High values imply a well confined donor layer, while lower values indicate that spreading has occurred. The Si spreading estimated from the SCC assuming a uniform distribution of the Si atoms is 35 ML.

The growth cycle for layer B684 allowed Si spreading towards the substrate to be differentiated from that in the growth direction. Since Si spreading is eliminated by growth at $T_s \leqslant 470\,^{\circ}\mathrm{C}$, any migration which occurred in B684 must have been caused by thermal diffusion into the substrate during the 16 s for the δ doping and the subsequent 300 s growth interrupt to decrease T_s to 470 °C. None should have taken place during the deposition of the 0.5 μm thick cap layer at 470 °C. As shown in Table I, the best fit to the experimental data is obtained by assuming a width of 2 ML in the SCC. No diffusion has occurred. In B685 however, the layers above the delta plane are grown at higher temperature, allowing surface segregation to occur. The result (Table I) is a dopant distribution 45 ML wide. The FFT amplitude spectra for B684 and B685 are shown in Fig. 2. The tighter confinement of the Si atoms in B684 compared with B685 is indicated by the shift of the $i \geqslant 1$ peaks to lower frequencies and an increase in the $n_{i=0}/n_{i=1}$ sub-band ratio from 1.87 to 2.66. Note that the Si spreading in B685 is higher even than that for B603, indicating a less confined doping profile caused possibly by a slightly higher growth temperature.

Strictly, any thermal diffusion which might have occurred during the growth of a 0.5 μm thick cap layer at 520 °C in B685 was not completely mimicked in sample B684. The additional sample, B713 was grown with a 15 min interrupt at 520 °C (equivalent in time to the growth of 0.25 μm of $In_{0.53}Ga_{0.47}As$ at 1.0 μm/h) following the deposition of the Si donors, to allow for the possibility of diffusion back from the growth surface towards the substrate, before the final 0.5 μm of undoped $In_{0.53}Ga_{0.47}As$ was deposited at 470 °C. Comparison of the SdH and SCC data suggests that near

TABLE I. Details of the main Si-doped $In_{0.53}Ga_{0.47}As$ samples considered in this study.

Sample	Type	Deposition T °C	Design n_s $\times 10^{16}$ m^{-2}	n_s $\times 10^{16}$ m^{-2}	n_H $\times 10^{16}$ m^{-2}	μ_s $m^2\,V^{-1}\,s^{-1}$	$\Delta\mu/\mu_s$	w (fitted) ML
B602	Delta	520	2.0	2.06	1.77	0.73	0.40	45
B618	Delta	420	2.0	2.15	1.66	0.69	0.54	2
B713	Delta	520 / 470	2.5	2.24	1.53	0.77	0.68	2
B603	Delta	520	3.0	3.14	2.46	0.69	0.53	35
B684	Delta	520 / 470	3.0	3.45	2.13	0.73	0.79	2
B685	Delta	470 / 520	3.0	3.12	2.64	0.66	0.46	45
B608	20 ML slab	520	8.0	8.64	7.46	0.49	0.40	
B644	20 ML slab	470	8.0	8.63	5.84	0.43	0.69	20
B696	Delta	420	15.0	14.84	8.55	0.35	0.86	2

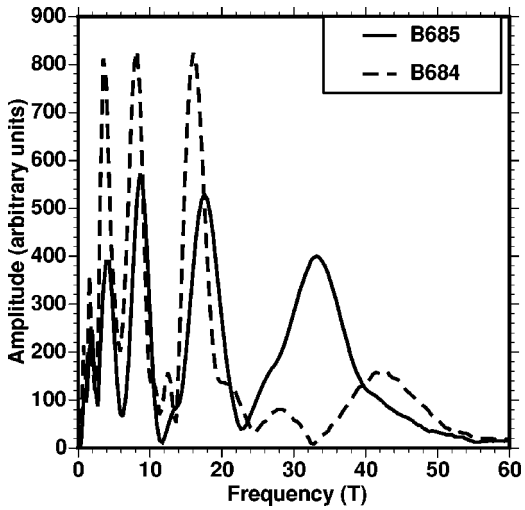

FIG. 2. Shubnikov–de Haas frequency data showing the differences between spectra for a strongly confined δ-layer sample (B684) and a sample in which the donors have spread (B685).

ideal δ doping was again achieved with an inferred spreading of 2 ML, and therefore that no diffusion had occurred during the extended period B713 was held at 520 °C. Abrupt confinement similar to that observed in B713 was also obtained from layer B618, doped to a comparable Si density $N_D \approx 2 \times 10^{12}\,\mathrm{cm}^{-2}$ at 420 °C and capped with 20 ML of undoped material at the same temperature before the final growth of 0.5 μm undoped $In_{0.53}Ga_{0.47}As$ at 520 °C. This shows that the substrate temperature during δ doping is not a critical factor in the growth cycle for achieving an abruptly confined doping profile in lattice matched InGaAs. In contrast, the fitted dopant widths for B602, similar to B618 but grown entirely at 520 °C, are 45 ML (UD) and 40 ML (GD).[15]

To summarize, the results for B684 and B713 show that diffusion of Si in $In_{0.53}Ga_{0.47}As$ at temperatures below 520 °C is negligible. Significant spreading of Si in $In_{0.53}Ga_{0.47}As$ away from the δ-doped plane only takes place when the δ layer is covered with additional material and the wafer temperature exceeds 470 °C (layers B603, B685, and B602). The only requisite condition for achieving an ideal δ-doping profile in lattice matched InGaAs is the growth of a thin cap layer of undoped material at low substrate temperature $T_s \leqslant 470$ °C after the deposition of the Si atoms. The dopant width does not depend on the substrate temperature during the incorporation of the Si atoms on the nongrowing surface of the material. This is compelling evidence for Si spreading only by surface segregation (at least at temperatures up to 520 °C). We have confirmed these deductions from SdH measurements and SCC by growing a special sample containing multiple δ-doped layers grown at different T_s values, and analyzing it using SIMS. The results confirm, to the resolution of the SIMS technique, that low T_s layers remain confined, but that layers deposited at 520 °C show an asymmetric, broadened profile with spreading of the Si dopants in the growth direction, as expected for surface segregation.

B. Limits to the three-band Kane model

The slab-doped samples B644 and B608 were grown to extend the study of the incorporation of a controlled doping profile into $In_{0.53}Ga_{0.47}As$ at higher doping densities. The layer structures of both samples consisting of $8 \times 10^{12}\,\mathrm{cm}^{-2}$ Si atoms distributed uniformly through 20 ML and grown at 470 °C (B644) and 520 °C (B608) are shown in Figs. 1(c) and 1(d). Shubnikov–de Haas measurements for B644 were performed using the 50 T pulsed magnetic field system because the $i=0$ subband, due to its relatively low mobility, was not resolved in the FFT spectrum within the 13 T field range of the superconducting magnet. At this high doping density a satisfactory fit between theory and experiment is not achieved for the 20 ML slab grown at 520 °C (B608) if a uniform distribution of the Si donors is assumed, suggesting an asymmetry of the doping profile. Pronounced differences between the subband densities deduced from experiment and theory were found even when a comparison with a much broadened uniform doping profile was attempted. In contrast the reduction in T_s from 520 to 470 °C (B644) suppressed the Si spreading and created the intended 20 ML uniform distibution of Si donors. The excellent agreement between the SdH measurements and the SCC for a width of 20 ML is shown in Table II. In B644, the temperature was kept at 470 °C during the growth of the 20 ML thin slab and of 30 ML of undoped material at either side of the doped region. Once more the profile is unaffected by the final growth of the

TABLE II. Theoretical fits to experimental subband densities for two samples. The well widths assumed for the fits are 20 ML for B644 and 2 ML for B696.

	Sample B644			Sample B696	
Subband No.	Measured n_s $\times 10^{16}$ m^{-2}	Fitted n_s $\times 10^{16}$ m^{-2}	Subband No.	Measured n_s $\times 10^{16}$ m^{-2}	Fitted n_s $\times 10^{16}$ m^{-2}
0	4.51	4.490	0	8.13	8.014
1	2.21	2.190	1	3.63	3.538
2	1.10	1.080	2	1.81	1.867
3	0.50	0.518	3	0.80	0.895
4	0.21	0.224	4	0.34	0.434
5	0.10	0.082	5	0.15	0.176
6		0.015	6		0.064
			7		0.010
Total	8.63	8.60	Total	14.86	15.00

0.5 μm cap layer at 520 °C, showing that a preferential migration of the Si donors towards the growth front is the principal mechanism contributing to the redistribution of Si for $T_s \approx 520$ °C.

For both the layers B608 and B644 the total carrier density measured from the SdH effect was $\approx 8.6\times10^{12}\,\mathrm{cm}^{-2}$ which in the case of B644 is equivalent to a bulk density of $1.5\times10^{19}\,\mathrm{cm}^{-3}$. The Fermi energy predicted by the SCC for a total carrier density of $8.5\times10^{12}\,\mathrm{cm}^{-2}$ Si donors distributed uniformly into 20 ML is 250 meV above the Γ-conduction band minimum and well below the energy of the L-conduction band minimum ($E_{\Gamma\text{-}L}=550$ meV) making the three-band Kane model a reasonable approximation to adopt at this density. Self-consistent calculations based on the three-band Kane model for $1.7\times10^{13}\,\mathrm{cm}^{-2}$ Si donors uniformly distributed in 2 ML, however, predict a Fermi energy of 550 meV, equal to the separation between the Γ- and L-conduction band minima. Layer B696 was δ doped at $1.5\times10^{13}\,\mathrm{cm}^{-2}$, and grown at 420 °C, to assess how accurately the Kane model describes the electronic properties of a δ layer at very high doping densities. The low growth temperature was used to eliminate any possible enhancement of Si spreading at the high doping densities studied. Judging by the mean separation of the atoms,[19] the equivalent three-dimensional doping density is similar to the maximum that has been achieved to date with bulk InGaAs layers grown lattice matched to InP by MBE ($6\times10^{19}\,\mathrm{cm}^{-3}$ at $T_s \approx 370$ °C).[20] As with layer B644 the $i=0$ subband of B696 was not resolved within the 13 T range of the superconducting magnet and the 50 T pulsed magnetic field system was used. The electron populations for the six occupied subbands observed are compared with theoretical predictions of SCC based on the three-band Kane model, assuming a uniform distribution of silicon donors in 2 ML, in Table II. Agreement between theory and experiment is remarkably good. We therefore conclude that, even for electron densities as high as $1.5\times10^{13}\,\mathrm{cm}^{-2}$, the $i=0$ subband at the L minimum is not populated and the three-band Kane model is adequate to describe the band structure.

C. The mobility of carriers in InGaAs δ-doped layers

As can be readily seen from Table I, for all slab- and δ-doped layers, the electron concentrations derived from the Hall measurements (n_H) are lower than the sums of the individual sub-band densities deduced from the FFT analysis of the Shubnikov–de Haas data (n_s). This striking result can be directly attributed to the different mobilities of the electronic sub-bands. At high Si doping densities ionized-impurity scattering is the dominant scattering mechanism at low temperatures and the different spatial overlap of the subband wave functions with the ionized donors is reflected in the different sub-band mobilities. Whenever the mobilities in the individual sub-bands of a multi-sub-band system differ, then necessarily the Hall mobility will be higher than the transport mobility deduced from SdH measurements and the corresponding effective carrier concentration will be lower. We first prove this result.

We start from the usual low field expression for the Hall coefficient for a multi-sub-band system,

$$R_H e = \frac{\sum_i n_i \mu_i^2}{\sum_i (n_i \mu_i)^2}, \tag{3.1}$$

where the sum is over all the occupied sub-bands, μ_i is the mobility of the electrons at the Fermi level in the ith subband, and we have ignored the carrier sign. The Hall carrier concentration is given by the reciprocal of $R_H e$ while the true carrier concentration measured by the SdH effect is given by

$$n_s = \sum_i n_i . \tag{3.2}$$

Consider the inequality

$$\sum_{i,j} n_i n_j (\mu_i - \mu_j)^2 > 0, \tag{3.3}$$

where both i and j range across all subbands. For $i \neq j$ this inequality must be true as all the terms are positive and we can add in the terms for the same subband, which are zero, without violating the inequality. Expanding and rearranging we get

$$\sum_{i,j} n_i n_j (\mu_i^2 + \mu_j^2) > 2 \sum_{i,j} \mu_i \mu_j n_i n_j . \tag{3.4}$$

As i and j are dummy suffices, we can rearrange Eq. (3.4) to get

$$2 \sum_i n_i \mu_i^2 \sum_j n_j > 2 \sum_i n_i \mu_i \sum_j n_j \mu_j \tag{3.5}$$

or

$$\sum_i n_i > \frac{\left(\sum_i n_i \mu_i \right)^2}{\sum_i n_i \mu_i^2}. \tag{3.6}$$

Equation (3.6) is exactly the result we require, $n_s > n_H$. It is known for two subbands[21,22] but has not been proved as a general result for any number of occupied subbands (n_i, μ_i).

We may now use the difference between n_s and n_H to obtain information about the distribution of mobilities over the sub-bands. We define the mean transport mobility

$$\mu_s = \frac{\sigma}{n_s e} = \frac{\sum_i n_i \mu_i}{\sum_i n_i} \tag{3.7}$$

and the effective Hall mobility

$$\mu_H = \frac{\sigma}{n_H e} = \sigma R_H = \frac{\sum_i n_i \mu_i^2}{\sum_i n_i \mu_i}. \tag{3.8}$$

As expected,

$$n_s\mu_s = n_H\mu_H . \tag{3.9}$$

We define the variance of the mobility for the electrons in all sub-bands in the usual way as

$$\Delta\mu^2 = \frac{\sum_i n_i(\mu_i-\mu_s)^2}{\sum_i n_i} = \frac{\sum_i n_i\mu_i^2}{\sum_i n_i} - \mu_s^2 . \tag{3.10}$$

Normalizing this to the mean mobility and substituting from Eq. (3.8) we obtain

$$\frac{\Delta\mu^2}{\mu_s^2} = \frac{n_s}{n_H} - 1 = \frac{\mu_H}{\mu_s} - 1. \tag{3.11}$$

Thus the ratio of the two measured carrier concentrations or mobilities gives the normalized variance of the mobility over the sub-bands. Unless the mobilities in all subbands are equal (and hence the variance $\Delta\mu^2$ is zero), Eq. (3.11) implies that low magnetic field Hall measurements underestimate the total carrier concentration in a multi-sub-band system. A similar conclusion was reached by Gossmann and Unterwald[23] in studies of transport in Sb δ-doped layers on Si (100). They showed that the Hall effect underestimated the carrier concentration in isolated dopant layers, but not when the layers were brought close enough together to destroy the two-dimensional confinement.

Individual measurements of n_s and n_H, the mean mobility and the normalized standard deviation of mobility are given for all the samples in Table I. The mean mobility is plotted against total carrier concentration in Fig. 3(a) and shows a slow decline over our range of measurements. Such a slow decline is predicted by theoretical calculations of scattering in δ layers such as that of Hai, Studart, and Peeters[24] and Henriques.[25] Unfortunately calculations are not available for the $In_{0.53}Ga_{0.47}As$ system to enable quantitative comparisons to be made.

The sample pairs B602/B618, B603/B713, B685/B684, and B608/B644 have approximately the same number of Si atoms but differ in their growth temperatures and hence in the final width of the dopant distributions. Only small differences in mean mobility are found between the strongly confined samples and the less well confined samples of each pair [Fig. 3(a)]. However, the samples with the narrower doping profile do show a significantly higher ratio of n_s to n_H, and hence a greater standard deviation of mobility. This point is emphasized in Fig. 3(b) where the normalized standard deviation is plotted against carrier concentration for the samples in Table I and a number of other samples. The low growth temperature, more confined samples occupy a band above the high growth temperature less confined sample group, in which the donors have spread.

This striking result is not difficult to explain. In a multi-sub-band system, for the same total free electron density, the narrower the doping profile the deeper the effective confinement potential. The ground state is especially strongly confined in a region close to the donors, the electrons within it will be strongly scattered and their mobility is expected to be

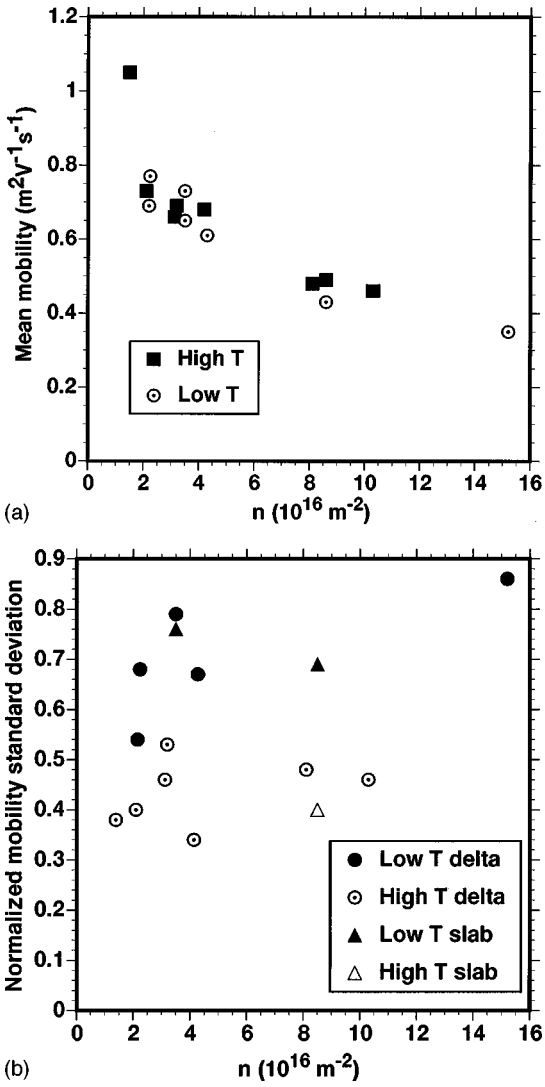

FIG. 3. (a) The mean mobilities (μ_s) for samples of different carrier concentrations. All samples from Table I and some others are included. High T implies growth of the layer directly above the dopant at 520 °C, low T implies growth at 470 °C or below. (b) The normalized standard deviations of mobility ($\Delta\mu/\mu_s$) for samples of (a) showing the significantly higher values observed for low T, strongly confined samples.

low compared with that of electrons in the higher, less confined subbands. This will result in a larger variance than for less closely confined doping layers. Thus although the phenomenon is not unexpected, the fact that it can be so clearly seen in the mobility data is a striking confirmation of the internal consistency of this data. This type of behavior is also predicted for the standard deviation of mobility calculated for Si δ-doped GaAs by Hai, Studart, and Peeters[24] and Henriques.[25] Hai, Studart and Peeters have calculated the subband mobilities for slab-doped wells as a function of doping thickness for $2\times10^{12}\,cm^{-2}$ carriers (three subbands occupied) and $8\times10^{12}\,cm^{-2}$ (four subbands occupied). For the former case, the normalized mobility variance decreases from 0.84 in the limit of zero thickness to 0.30 at 10 nm (35 ML). For the latter, the decrease is from 0.70 to 0.43. The equivalent values predicted by Henriques are 0.81 and 0.73 for ideal monolayers of $2\times10^{12}\,cm^{-2}$ and $8\times10^{12}\,cm^{-2}$ Si donors in GaAs, respectively, and 0.33 for $5\times10^{12}\,cm^{-2}$ Si

donors distributed uniformly in 11 nm (40 ML). These values are very similar to those we observe experimentally for similar changes in width.

This impressive agreement between theory[24–26] and our experimental data confirms, as is shown in our mathematical analysis, that the increasing discrepancy between n_H and n_s in wells with the same doping density but with progressive confinement of the donors to form an ideal monolayer distribution, is a direct consequence of the increasing differences in sub-band mobilities. In addition our analysis is applicable to any confined doping profile, irrespective of material. It is not limited to Si δ-doped $In_{0.53}Ga_{0.47}As$ but, as noted above, also applies to the low field Hall measurements on Sb δ-doped Si films by Gossmann and Unterwald[23] and to measurements on Si δ-doped GaAs.[27]

Various methods are available, using further information, to deduce individual sub-band mobilities. The nonlinear higher field longitudinal and transverse resistivity data can be interpreted to give information about the transport mobilities for the individual sub-bands; the most sophisticated method of this type is the mobility spectrum technique of Beck and Anderson.[28] From the damping of the SdH oscillations, analyzed either using the Dingle plots[29,30] or from the shape of the peaks in the FFT spectra,[11] quantum subband mobilities can be deduced. It is not our intention in this paper to go beyond the results we have already reported from the linear regime. However, the data for such a study is available and will be presented in a future paper.

IV. CONCLUSIONS

The Si spreading in δ- and slab-doped lattice matched InGaAs on InP by MBE has been studied on epitaxial layers with unique structures and growth temperature profiles to differentiate between thermal diffusion and surface segregation. Compelling evidence for preferential migration of the Si donors in the growth direction was presented for growth temperatures $T_s \geqslant 470\,^{\circ}\mathrm{C}$. Thermal diffusion is negligible for substrate temperatures $T_s \leqslant 520\,^{\circ}\mathrm{C}$. The three-band Kane model describes adequately the electronic properties of δ-doped layers with doping densities as high as $1.5 \times 10^{13}\,\mathrm{cm}^{-2}$ and Fermi energies slightly lower than the energy separation between the Γ- and L-conduction band minima. Direct comparison of the total free electron concentration derived from the FFT analysis of the SdH data with the carrier concentration measured from low magnetic field Hall measurements shows that the significant decrease of the free electron concentration deduced from the Hall measurements is associated with the confinement of the Si donors and can be attributed to the different mobilities of the different occupied subbands. It is found that the more confined the doping profile for the same Si doping density the higher is the discrepancy between nominal Hall and SdH carrier concentrations; this is consistent with the greater differences in mobility between subbands to be expected for narrower doping profiles.

ACKNOWLEDGMENT

This work was supported by the EPSRC of the U.K.

*Email: arlong@elec.gla.ac.uk
†Present address: VG Semicon, Imberhorne Lane, East Grinstead, West Sussex RH19 1XZ, U.K.

[1] S.J. Bass, J. Cryst. Growth **47**, 613 (1979).
[2] C.E.C. Wood, G. Metze, J. Berry, and L. F. Eastman, J. Appl. Phys. **51**, 383 (1980).
[3] E.F. Schubert, in *Delta Doping of Semiconductors*, edited by E.F. Schubert (Cambridge University Press, Cambridge, 1995).
[4] H.-J. Gossmann, in *Delta Doping of Semiconductors* (Ref. 3).
[5] J.J. Harris, J. Mater. Sci.: Mater. Electron. **4**, 93 (1993).
[6] E.F. Schubert, J.B. Stark, B. Ullrich, and J.E. Cunningham, Appl. Phys. Lett. **57**, 497 (1990).
[7] J.J. Harris, D.E. Ashenford, C.T. Foxon, P.J. Dobson, and B.A. Joyce, Appl. Phys. A: Solids Surf. **33**, 87 (1984).
[8] E.F. Schubert, R.F. Kopf, J.M. Kuo, H.S. Luftman, and P. Gabrinski, Appl. Phys. Lett. **54**, 2091 (1988).
[9] R.B. Beall, J.B. Clegg, and J.J. Harris, Semicond. Sci. Technol. **3**, 612 (1988).
[10] A. Zrenner, F. Koch, and K. Ploog, Surf. Sci. **196**, 671 (1988).
[11] E. Skuras, R. Kumar, R.L. Williams, R.A. Stradling, J.E. Dmochowski, E.A. Johnson, A. Mackinnon, J.J. Harris, R.B. Beall, C. Skierbiszewski, J. Singleton, P.J. van der Wel, and B.P. Wisniewski, Semicond. Sci. Technol. **6**, 535 (1991).
[12] P.M. Koenraad, A.C.L. Hessels, F.A.P. Blom, J.A.A.J. Perenboom, and J.H. Wolter, Physica B **184**, 221 (1993).
[13] G. Nachtwei, S. Heide, H. Kunzel, and W. Passenberg, J. Phys.: Condens. Matter **5**, 1091 (1993).
[14] W-P. Hong, F. DeRosa, R. Bhat, S.J. Allen, and J.R. Hayes, Appl. Phys. Lett. **54**, 457 (1989).
[15] M. McElhinney, B. Vögele, M.C. Holland, C.R. Stanley, E. Skuras, A.R. Long, and E.A. Johnson, Appl. Phys. Lett. **68**, 940 (1996).
[16] B. Vögele, C.R. Stanley, E. Skuras, A.R. Long, and E.A. Johnson, J. Cryst. Growth **175/176**, 229 (1997).
[17] H. Jones, R.G. Jenkins, M. van Kleemput, R.J. Nicholas, W.J. Siertsma, and M. van der Burgt, Physica B **201**, 546 (1994).
[18] E.A. Johnson and A. MacKinnon, Semicond. Sci. Technol. **5**, S189 (1990).
[19] E.F. Schubert, J.E. Cunningham, and W.T. Tsang, Solid State Commun. **63**, 591 (1987).
[20] T. Fujii, T. Inata, K. Ishii, and S. Hiyamizu, Electron. Lett. **22**, 191 (1986).
[21] R.L. Williams, P. Coleridge, Z.R. Wasilewski, M. Dion, A. Sachrajda, and S. Rolfe, Solid State Commun. **78**, 493 (1991).
[22] J. Chen, H.H. Wieder, and A.P. Young, J. Appl. Phys. **76**, 4743 (1994).
[23] H.-J. Gossmann and F.C. Unterwald, Phys. Rev. B **47**, 12 618 (1993).
[24] G.Q. Hai, N. Studart, and F.M. Peeters, Phys. Rev. B **52**, 8363 (1995).
[25] A.B. Henriques, Phys. Rev. B **53**, 16 365 (1996).
[26] L.R. Gonzalez, J. Krupski, and T. Szwacka, Phys. Rev. B **49**, 11 111 (1994).
[27] A. Zrenner, F. Koch, R.L. Williams, R.A. Stradling, K. Ploog, and G. Weimann, Semicond. Sci. Technol. **3**, 1203 (1988).
[28] W.A. Beck and J.R. Anderson, J. Appl. Phys. **62**, 541 (1987).
[29] S. Yamada and T. Makimoto, Appl. Phys. Lett. **57**, 1022 (1990).
[30] P.M. Koenraad, in *Delta Doping of Semiconductors* (Ref. 3).